Journal of Hazardous Materials 217–218 (2012) 217–223

Contents lists available at SciVerse ScienceDirect

# Journal of Hazardous Materials

journal homepage: www.elsevier.com/locate/jhazmat

# Formation of chlorinated by-products during photo-Fenton degradation of pyrimethanil under saline conditions. Influence on toxicity and biodegradability

Carla Sirtori [a,b,c,*], Ana Zapata [a], Sixto Malato [a,d], Ana Agüera [b,d]

[a] Plataforma Solar de Almería (CIEMAT), Carretera Senés, km 4, 04200 Tabernas, Almería, Spain
[b] Pesticide Residue Research Group, University of Almería, 04120 Almería, Spain
[c] Universidade Federal da Integração Latino-Americana (UNILA), Av. Tancredo Neves, 6731 - Bloco 4, Caixa Postal 2044, CEP 85867-970, Foz do Iguaçu PR, Brazil
[d] CIESOL, Joint Centre University of Almeria-CIEMAT, 04120 Almería, Spain

ARTICLE INFO

*Article history:*
Received 20 November 2011
Received in revised form 4 March 2012
Accepted 6 March 2012
Available online 15 March 2012

*Keywords:*
Pyrimethanil
Photo-Fenton
Chlorinated transformation products
LC–TOF-MS

ABSTRACT

This study evaluated the formation of chlorinated transformation products during photo-Fenton treatment of pyrimethanil (PYR-20 mg $L^{-1}$) in two water matrices, demineralised water (DW) and water containing 5 g $L^{-1}$ of NaCl ($DW_{NaCl}$). All experiments were carried out in compound parabolic collectors (CPC) at an initial $Fe^{2+}$ concentration of 5 mg $L^{-1}$ and $H_2O_2$ concentration of 150–350 mg $L^{-1}$. Dissolved Organic Carbon (DOC), High-Performance Liquid Chromatography with Diode-Array Detection (HPLC–DAD), Liquid Chromatography–Time-Of-Flight Mass Spectrometry (LC–TOF-MS), toxicity and biodegradability tests were conducted to control the photocatalytic treatment. In DW, PYR was completely eliminated after 11.8 min of illumination and initial DOC was reduced 50% after 79 min of illumination with 33 mM of $H_2O_2$ consumed. On the other hand, in $DW_{NaCl}$ water matrix, the same reduction in DOC took 110 min of illumination and $H_2O_2$ consumption of 39 mM, and total degradation of PYR was observed at 12 min of illumination. PYR transformation products (TPs) were identified by LC–TOF-MS. It was demonstrated that photo-Fenton in a $DW_{NaCl}$ produces some chlorinated TPs in addition to the non-chlorinated TPs identified during degradation in the DW. All TPs formed were eliminated during photo-Fenton. Additionally, the presence of chlorinated TPs does not increase the toxicity of the water, and TPs formed are more biodegradable than PYR.



## 1. Introduction

The expansion of agriculture, mainly due to the widespread use of pesticides, has contributed directly to water pollution. The most important pesticide pollution pathways into the environment are diffuse contamination and surface run-off [1]. The increase in the occurrence and abundance of these compounds in natural water has caused some countries to regulate pesticides to prevent their toxic effects on ecosystems. EU legislation, especially the Water Framework Directive (WFD), and other complementary European Directives, limit the concentrations of hazardous chemical substances, such as pesticides and others priority chemicals, in bodies of water [2]. The latest Directive, approved in 2008 (2008/105/EC), includes environmental quality standards (EQS: annual averages and maximum allowable concentrations) for priority substances and certain other pollutants to improve surface water chemical status. It also includes dioxins and PCBs in the list of substances subject to review in 2011 for possible identification as priority substances or priority hazardous substances [3].

Pesticides present generally have high chemical stability, and are usually resistant to conventional biological processes, demonstrating the necessity to develop new treatment alternatives. In this context, advanced oxidation processes (AOPs) are effective new technologies able to eliminate stable and recalcitrant compounds. AOPs are characterized by the production of hydroxyl radicals ($^{\bullet}OH$), which are powerful, unselective oxidants (2.8 V vs. standard hydrogen electrode). Recent studies confirm the potential of these processes for transforming toxic or recalcitrant compounds, such as pesticides, into biodegradable substances susceptible to elimination in a following biological treatment [4]. This reduces the cost of reagents (i.e., $H_2O_2$, $Fe^{2+}$, $TiO_2$), energy consumption and reactor dimensions associated with the full AOP treatment, which is shortened to a minimum.

Depending on the transformation during the AOP, not only the active substances must be analysed, but also the transformation products (TPs) generated during the treatment. An IUPAC technical report on regulatory limits for pesticide residues in water [5] states that if a TP has been identified in amounts exceeding 10% of the applied dose of a pesticide, it should be considered a major degradation product and included in an additional risk assessment. The

* Corresponding author at: Universidade Federal da Integração Latino-Americana (UNILA), Av. Tancredo Neves, 6731 - Bloco 4, Caixa Postal 2044, CEP 85867-970, Foz do Iguaçu PR, Brazil. Tel.: +55 45 3576 7307; fax: +55 45 3576 7306.
*E-mail addresses:* carla.sirtori@unila.edu.br, carla.sirtori@psa.es (C. Sirtori).

0304-3894/$ – see front matter © 2012 Elsevier B.V. All rights reserved.
doi:10.1016/j.jhazmat.2012.03.017

report took specific information on TP pesticide activity, toxicology and ecotoxicology into account.

In addition, when the inorganic content in the water matrix is very high, some reactive species like chloride or sulphate radicals are produced, which directly influence the TPs generated during the AOP. Chlorine radicals ($Cl^{\bullet}$) may lead to the formation of chlorinated organic compounds, which are known to be very harmful, and in some cases, able to generate persistent substances. To date, few studies have been published reporting on the formation of intermediate chlorinated degradation products [6–8], which must therefore be the subject of further study.

Pyrimethanil (PYR), N-(4,6-dimethylpyrimidin-2-yl)-aniline, is an anilinopyrimidine employed as a fungicide in agriculture. Some studies have related the potential danger of PYR to an increase in liver weight. Histopathological changes in liver and thyroid have been observed in short-term toxicity studies in rats and mice [9]. However, this pesticide is not included in the priority chemical substances list. The study of this compound in degradation studies is urged by its widespread use in agriculture for the prevention of botrytis (greenhouses, vineyards, etc.). Additionally, this pesticide is commonly used in intensive agriculture in the southeast of Spain [10,11].

The main purpose of this study was to determine whether PYR chlorinated TPs are formed during photo-Fenton in a matrix with high chloride content. To ensure the quality of the results, the same experimental and analytical procedures were applied to PYR degradation in both demineralised water (DW) and in water containing 5 g $L^{-1}$ of NaCl ($DW_{NaCl}$). Three samples containing variable amounts of PYR and chlorinated TPs were analysed by respirometry to evaluate the changes in toxicity and biodegradability during photodegradation in saline conditions. Another aim was to find out if there is any biotransformation of PYR and its TPs after 24 h of exposure to activated sludge.

## 2. Experimental

### 2.1. Chemicals

The 99.9% pure PYR standard CAS number 53112-28-0 was provided by Riedel-de Haën (Germany). PYR degradation was evaluated in two different water matrices, demineralised water (DW) supplied by the Plataforma Solar de Almería (PSA) demineralisation plant (conductivity <10 μS $cm^{-1}$, $Cl^-$ 1.2–1.3 mg $L^{-1}$, $NO_3^-$ < 0.2 mg $L^{-1}$, organic carbon < 0.5 mg $L^{-1}$) and saline water with 5 g $L^{-1}$ of NaCl ($DW_{NaCl}$). For chromatographic analysis, HPLC-grade methanol was supplied by Merck (Germany); Milli-Q ultra-pure water system from Millipore (Milford, MA, USA) and formic acid (purity, 98%) from Fluka were used. All photo-Fenton experiments were performed using iron sulphate heptahydrate ($FeSO_4 \cdot 7H_2O$), reagent-grade hydrogen peroxide (30%, w/v), and sulphuric acid for pH adjustment, all purchased from Panreac.

### 2.2. Analytical determinations

Mineralisation was monitored by measuring the dissolved organic carbon (DOC) by direct injection of filtered samples into a Shimadzu-5050A TOC analyzer with an NDIR detector calibrated with standard solutions of potassium phthalate. PYR degradation was evaluated by direct injection in an HPLC–DAD (Agilent Technologies, series 1100) equipped with a C-18 column (LUNA 5 μm, 3 mm × 150 mm, from Phenomenex) and operated at a flow rate of 0.5 mL $min^{-1}$. An isocratic method with 15% HPLC-grade acetonitrile and 85% ultrapure water (Millipore Co.) mobile phase was employed with detection at $\lambda$ = 210 nm. Total iron concentration was monitored by colorimetric determination with 1,10-phenanthroline, following ISO 6332, and using a Unicam-2 spectrophotometer. Hydrogen peroxide was analysed by a fast, simple spectrophotometric method using ammonium metavanadate, which allows the immediate determination of $H_2O_2$ concentration based on the formation of a red-orange peroxovanadium cation during $H_2O_2$ reaction with metavanadate [12].

TPs generated during photo-Fenton were monitored by LC–TOF-MS (Agilent Technologies). An HPLC Series 1100 system (Agilent Technologies) equipped with a 3 mm × 250 mm reverse-phase C18 analytical column, with 5 μm particle size packing (ZORBAX, SB-C18, Agilent Technologies) was used. The mobile phase was a mixture of acetonitrile acidified by 0.1% formic acid (A) and water acidified by 0.1% formic acid (B) at a flow rate of 0.4 mL $min^{-1}$. A linear gradient progressed from 10%A (initial conditions) to 100%A in 50 min, and was then kept at 100%A for 5 min. The 20-μL samples injected were previously filtered through Teflon. Biomass samples were centrifuged and extracted with acetonitrile (50/50). The HPLC system was connected to a TOF mass spectrometer (Agilent Technologies) equipped with an electrospray interface operating under the following conditions: capillary 4000 V, nebuliser 40 psi g, drying gas 9 L $min^{-1}$, gas temperature 300 °C, skimmer voltage 60 V, octapole rf 250 V, with four different fragmentation voltages, 190, 230, 260 and 300 V. Data were processed with MassHunter Workstation Software, selecting elemental composition, double-bond equivalent (DBE), electron state "even", and number of charges +1. In most cases, possible elemental compositions for ions were assigned with a deviation of 5 ppm.

Photo-Fenton experiments were performed in a compound parabolic collector (CPCs) pilot plant designed for solar photocatalytic applications. The reactor is composed of two modules of eight Pyrex glass tubes mounted on a fixed platform tilted 37° (local latitude). The total area is 3 $m^2$ and the total volume is 40 L, 22 of which are irradiated volume. The total volume in each experiment was 35 L. At the beginning of all the photocatalytic experiments (photoreactor covered to avoid any photoreaction during preparation), PYR standard solution was added directly to the photoreactor, and a sample was taken after 15 min of homogenisation (initial concentration, around 20 mg $L^{-1}$). After that, the pH was adjusted with sulphuric acid and another sample was taken after 15 min to confirm the pH. Then, iron salt was added ($FeSO_4 \cdot 7H_2O$) and homogenised well for 15 min before sampling. Finally the first dose of hydrogen peroxide was added, the photoreactor was uncovered and samples were taken at preset times to evaluate the degradation process.

Photo-Fenton experiments were carried out at a pH adjusted to 2.6–2.8 ($H_2SO_4$, 2N) with 5 mg $L^{-1}$ of $Fe^{2+}$. Initial hydrogen peroxide concentration was around 250 mg $L^{-1}$ and was kept at 150–350 mg $L^{-1}$ throughout the experiments. The concentration of $H_2O_2$ was maintained in this range by the addition of hydrogen peroxide during the treatment time at various reaction times. A sample was taken periodically to carry out the determination of hydrogen peroxide present in the solution. Solar ultraviolet radiation (UV) was measured by a global UV radiometer (KIPP&ZONEN, model CUV 3) mounted on a platform tilted to 37°, which provides data in terms of incident UV (W $m^{-2}$). This gives a measure of the energy reaching any surface in the same position with regard to the sun. With Eq. (1), combination of the data from several days' experiments and the comparison of photoreactors installed at different sites is possible.

$$t_{30\,\mathrm{W},n} = t_{30\,\mathrm{W},n-1} + \Delta t_n \frac{\mathrm{UV}}{V_\mathrm{T}};\ \Delta t_n = t_n - t_{n-1};\ t_0 = 0 (n = 1) \qquad (1)$$

where UV is the average solar ultraviolet radiation measured during $\Delta t_n$, $t_n$ is the experimental time for each sample, $V_\mathrm{T}$ is the total volume of water loaded in the pilot plant (35 L), $V_\mathrm{i}$ is the total irradiated volume (22 L, glass tubes) and $t_{30\,\mathrm{W}}$ is a "normalized illumination time", which refers to a constant solar UV power of 30 W $m^{-2}$ (typical solar UV power on a normal sunny day around noon).

### 2.3. Biological measurements

Respirometry assays were carried out using a BM-T respirometer (from Surcis SA) consisting of a 1-L capacity biological reactor with temperature control (to maintain the temperature at 20 °C by external circuit) and a Stratos 2402 Oxy oximeter. Respirometry is based on the consumption of oxygen by the microorganisms in the activated sludge, and its operation is based on closed-loop batch processing in which the dissolved oxygen contained in the sludge is continuously measured.

For toxicity and biodegradability analysis, the reactor was first loaded with activated sludge (700 mL) from the Almería (Spain) municipal wastewater treatment plant and the respirometer reactor flask was kept in continuous aeration and agitation to air saturation conditions. During this period, 3 mg of N-allylthiourea per gram of volatile solids (VSS) was added to the activated sludge to inhibit nitrification and measure the effect of the sample alone on the heterotrophic bacteria.

Toxicity was evaluated by comparing the bacterial activity in two assays: one containing the sludge and 300 mL of distilled water with sodium acetate (0.5 g/g VSS), a biodegradable substrate (reference), and another containing the sludge and 300 mL of the target sample with the same biodegradable substrate. Tests were extended until the biomass reached the maximum respiration rate ($Rs_{max}$, mg $L^{-1}$ $h^{-1}$). The percentage inhibition of each sample is expressed quantitatively according to the following equation:

$$I(\%) = 100 \times (1 - Rs_{max\,SAMPLE}/Rs_{max\,REFERENCE}) \quad (2)$$

For biodegradability measurements, 300 mL of each filtered sample were added to the respirometer reactor and oxygen consumption was monitored automatically. At the end of the test, the respirometer software gave the readily biodegradable fraction of the sample (rbCOD) based on the total oxygen consumption measured and the normal biomass growth rate calculated (0.67) for activated sludge from conventional municipal wastewater treatment plants. The rbCOD/COD ratio shows the sample's biodegradability, where 0.3 or higher means that it is classified as very biodegradable and 0.1 is biodegradable, whereas below 0.05 indicates that the sample is not biodegradable (0.05–0.1 is slightly biodegradable) [13].

The biodegradability tests lasted 24 h for two reasons. The main purpose was to observe the evolution of pyrimethanil and its TPs during contact with the activated sludge in order to evaluate possible biotransformation or formation of new TPs. Samples were analysed by LC–TOF-MS at the beginning and after 24 h of exposure to the biomass (both from supernatant and from solid activated sludge). The activated sludge was also analysed because previous experiments showed that PYR was partially adsorbed on the biomass [14], and therefore, TPs might also be adsorbed. For these analyses, the biomass was previously extracted with acetonitrile. The second goal was to evaluate any potentially chronic sample toxicity. After the tests, sodium acetate was added to check the ability of the biomass to consume an easily biodegradable compound after continuous exposure to the solutions containing PYR and its TPs.

## 3. Results and discussion

### 3.1. Pyrimethanil degradation

PYR degradation by photo-Fenton was evaluated in two water matrixes (DW and $DW_{NaCl}$) to study the formation and evolution of PYR and its TPs during the process, especially chlorinated TPs in $DW_{NaCl}$.

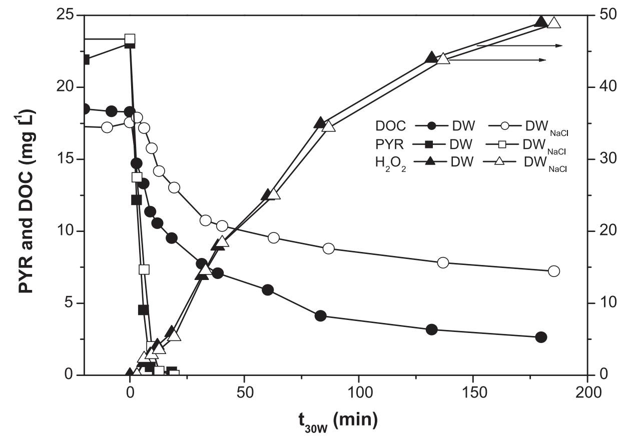


**Fig. 1.** DOC, PYR degradation and $H_2O_2$ consumption during photo-Fenton with 5 mg $L^{-1}$ of $Fe^{2+}$ in DW (solid dots) and $DW_{NaCl}$ (open dots).

The starting conditions (20 mg $L^{-1}$ PYR and 5 mg $L^{-1}$ $Fe^{2+}$) were adapted from previous photo-Fenton PYR degradation studies in specific industrial wastewater [10,14]. In general, 20 mg $L^{-1}$ PYR might be considered too high for diffuse contamination and surface run-off, but to unequivocally identify TPs, the initial concentration of the parent compound has to be high. Otherwise it would be nearly impossible to determine the TPs during treatment, since they are usually degraded as soon as they occur. In DW, 50% of the initial DOC was reduced after 79 min of illumination time with 33 mM of $H_2O_2$ consumed. PYR was completely eliminated after 11.8 min of illumination. In $DW_{NaCl}$, the same decrease in DOC took 110 min with an $H_2O_2$ consumption of 39 mM. PYR was also observed to be completely degraded at around 12 min of illumination time. These results are summarized in Fig. 1. Additionally, kinetic parameters of DOC mineralisation were evaluated for both water matrices. Pseudo first order constants ($k'_{ap}$) values were 0.02864 $min^{-1}$ and 0.02093 $min^{-1}$ for DW and $DW_{NaCl}$, respectively. Further, the maximum gradient of the degradation curve ($r_{DOC,0}$) was 18.2 mg $min^{-1}$ for DW and 19.3 mg $min^{-1}$ for $DW_{NaCl}$.

As observed, photo-Fenton degradation of PYR was less efficient in terms of DOC reduction in the presence of NaCl. A longer illumination and higher hydrogen peroxide dose were required for less mineralization. This is due to the two well-known negative effects of chloride ions on AOPs, formation of chloro-Fe(III) complexes that reduce the amount of active iron, and scavenging of hydroxyl radicals [15]. Nevertheless, these effects were not noticeable in PYR degradation since it was eliminated in both cases with a similar illumination time and $H_2O_2$ consumption. In the presence of high concentrations of $Cl^-$, chlorine radicals and radicals formed from the reaction between chlorine radicals and hydrogen peroxide could easily attack the original molecule, partly compensating the scavenging of $^\bullet OH$ by chloride (see reactions (I)–(III) described below) [14,16]. Furthermore, less active chloride radicals formed could also react with $H_2O_2$ (reactions (IV) and (V)) increasing the reagent consumption [17]. This demonstrated that the PYR molecule is susceptible to efficient degradation by the chloride radicals formed.

$$Cl^- + HO^\bullet \rightarrow ClOH^{\bullet -} \quad (I)$$

$$ClOH^{\bullet -} + H^+ \rightarrow Cl^\bullet + H_2O \quad (II)$$

$$Cl^\bullet + Cl^- \rightarrow Cl_2 \quad (III)$$

$$Cl^\bullet + H_2O_2 \rightarrow HO_2^\bullet + Cl^- + H^+ \quad (IV)$$

$$Cl_2^\bullet + H_2O_2 \rightarrow HO_2^\bullet + 2Cl^- + H^+ \quad (V)$$

**Table 1**
Accurate mass measurements determined by LC–TOF-MS for PYR and TPs generated during photo-Fenton treatment in both of the water matrices studied.

| Comp. | $R_t$ | Ion formula $[M+H]^+$ | Mass ($m/z$) | | Error (ppm) | DBE* | Water matrix |
|---|---|---|---|---|---|---|---|
| | | | Experimental | Calculated | | | |
| PYR | 23.3 | $C_{12}H_{14}N_3$ | 200.1187 | 200.1182 | −2.39 | 8 | DW, $DW_{NaCl}$ |
| | | $C_{12}H_{11}N_2$ | 183.0921 | 183.0917 | −2.34 | 9 | |
| | | $C_6H_7N_2$ | 107.0613 | 107.0604 | −8.73 | 5 | |
| P1 | 6.7 | $C_9H_{12}N_3O$ | 178.0905 | 178.0902 | −1.39 | 6 | DW, $DW_{NaCl}$ |
| | | $C_7H_{10}N_3$ | 136.0797 | 136.0797 | −0.38 | 5 | |
| | | $C_7H_7N_2$ | 119.0525 | 119.0531 | 4.7 | 6 | |
| | | $C_6H_5N_2$ | 105.0369 | 105.0375 | 5.62 | 6 | |
| | | $C_6H_8N$ | 94.0653 | 94.0651 | −11.54 | 4 | |
| P2 | 10.6 | $C_{12}H_{16}N_3O_3$ | 250.1192 | 250.1186 | −2.34 | 7 | DW, $DW_{NaCl}$ |
| | | $C_{12}H_{14}N_3O_2$ | 232.1056 | 232.1080 | 10.17 | 8 | |
| | | $C_{10}H_{14}N_3O_2$ | 207.1002 | 207.1007 | 2.35 | 6 | |
| | | $C_{10}H_{12}N_3O$ | 190.0989 | 190.0975 | −7.46 | 7 | |
| | | $C_8H_8N_3O$ | 162.0672 | 162.0662 | −6.28 | 7 | |
| | | $C_7H_{10}N_3$ | 136.0863 | 136.0869 | 4.3 | 5 | |
| | | $C_7H_7N_2$ | 119.0613 | 119.0604 | −7.84 | 6 | |
| | | $C_6H_5N_2$ | 105.0454 | 105.0447 | −6.49 | 6 | |
| P3 | 16.5 | $C_{12}H_{12}N_3O_2$ | 230.0937 | 230.0924 | −5.66 | 9 | DW, $DW_{NaCl}$ |
| | | $C_{12}H_{10}N_3O$ | 212.0829 | 212.0818 | −5.37 | 10 | |
| | | $C_{11}H_{10}N_3O$ | 200.0838 | 200.0818 | −9.85 | 9 | |
| | | $C_{11}H_{10}N_3$ | 184.0871 | 184.0869 | −0.7 | 9 | |
| | | $C_{10}H_{10}N_3$ | 172.0869 | 172.0869 | −0.05 | 8 | |
| P4 | 17.4 | $C_{12}H_{12}N_3O_2$ | 230.0929 | 230.0924 | −2.17 | 9 | DW, $DW_{NaCl}$ |
| | | $C_{10}H_{10}N_3$ | 172.0866 | 172.0869 | 1.88 | 8 | |
| | | $C_6H_7N_2$ | 107.0616 | 107.0604 | −11.55 | 5 | |
| P5 | 18.0 | $C_{12}H_{14}N_3O$ | 216.1147 | 216.1131 | −7.26 | 8 | DW, $DW_{NaCl}$ |
| | | $C_{11}H_9N_2$ | 169.075 | 169.076 | 6.38 | 9 | |
| P6 | 19.8 | $C_{12}H_{14}N_3O$ | 216.1138 | 216.1131 | −3.08 | 8 | DW, $DW_{NaCl}$ |
| | | $C_{12}H_{12}N_3$ | 198.1028 | 198.1026 | −1.15 | 9 | |
| | | $C_{11}H_{12}N_3$ | 186.1032 | 186.1026 | −3.34 | 8 | |
| | | $C_{11}H_{11}N_2$ | 171.0928 | 171.0917 | −6.62 | 8 | |
| | | $C_8H_7N_2$ | 131.0603 | 131.0604 | 0.28 | 7 | |
| | | $C_6H_4N$ | 90.0342 | 90.0338 | −4.24 | 6 | |
| P7 | 18.4 | $C_6H_9ClN_3$ | 158.0473 | 158.048 | 3.99 | 4 | $DW_{NaCl}$ |
| | | $C_6H_6ClN_2$ | 141.0213 | 141.0214 | 0.78 | 5 | |
| | | $C_5H_7ClN$ | 116.025 | 116.0262 | 9.97 | 3 | |
| | | $C_5H_6N$ | 80.0498 | 80.0495 | −4.58 | 4 | |
| P8 | 28.7 | $C_{12}H_{13}ClN_3$ | 233.0707 | 233.072 | 5.43 | 8 | $DW_{NaCl}$ |
| | | $C_{12}H_{10}ClN_2$ | 217.0523 | 217.0527 | 1.86 | 9 | |
| | | $C_{12}H_{12}N_3$ | 198.1029 | 198.1026 | −1.65 | 9 | |
| | | $C_7H_6N_2$ | 118.0563 | 118.0565 | 1.15 | 5 | |
| | | $C_5H_8N$ | 82.058 | 82.0579 | −2.32 | 3 | |
| P9 | 29.7 | $C_{12}H_{13}ClN_3$ | 233.0723 | 233.072 | −1.43 | 8 | $DW_{NaCl}$ |
| | | $C_{12}H_{10}ClN_2$ | 217.0544 | 217.0527 | −8 | 9 | |
| | | $C_{12}H_{12}N_3$ | 198.1022 | 198.1026 | 1.9 | 9 | |
| | | $C_9H_8N_3$ | 158.0718 | 158.0713 | −3.53 | 8 | |
| | | $C_7H_6N_2$ | 118.0534 | 118.0565 | 7.18 | 5 | |
| | | $C_5H_8N$ | 82.066 | 82.0651 | −10.17 | 3 | |
| P10 | 31.4 | $C_{12}H_{13}ClN_3$ | 233.0719 | 233.072 | 0.34 | 8 | $DW_{NaCl}$ |
| | | $C_{12}H_{10}ClN_2$ | 217.0516 | 217.0527 | 5.1 | 9 | |
| | | $C_{12}H_9N_2$ | 181.076 | 181.076 | 0.1 | 10 | |
| | | $C_{11}H_7N_2$ | 167.0599 | 167.0604 | 3.14 | 10 | |
| | | $C_{11}H_8N$ | 154.0644 | 154.0651 | 4.73 | 9 | |
| | | $C_6H_6ClN_2$ | 141.0219 | 141.0214 | −2.3 | 5 | |
| | | $C_5H_7ClN$ | 116.0255 | 116.0189 | 5.94 | 3 | |
| | | $C_5H_6N$ | 80.0496 | 80.0495 | −1.68 | 4 | |

### *3.2. Photocatalytic PYR TPs detected by LC–TOF-MS*

Samples from each experiment were analysed by LC–TOF-MS in full-scan, positive mode to detect the PYR TPs. The appearance of peaks with an appearance-disappearance time profile indicated possible TPs. Table 1 summarizes the analytical information relative to the TPs identified, such as calculated and experimental accurate masses of the protonated ions $[M+H]^+$, their respective errors in ppm and double bond equivalents (DBE) provided by the software. In addition, the low errors observed (mostly below 5 ppm), allowed correct assignation of the elemental composition of the ions.

Table 1 shows the ten TPs found in the matrices studied, six in DW (P1–P6) and ten in $DW_{NaCl}$ (P1–P10). Different experimental conditions and four fragmentation voltages (190, 230, 260 and 300 V) were applied during LC–TOF-MS analyses to find adequate in-source fragmentation for reliable identification.

As shown in Scheme 1, electrophilic substitution of one hydrogen atom in the PYR molecule by hydroxyl radicals constitutes

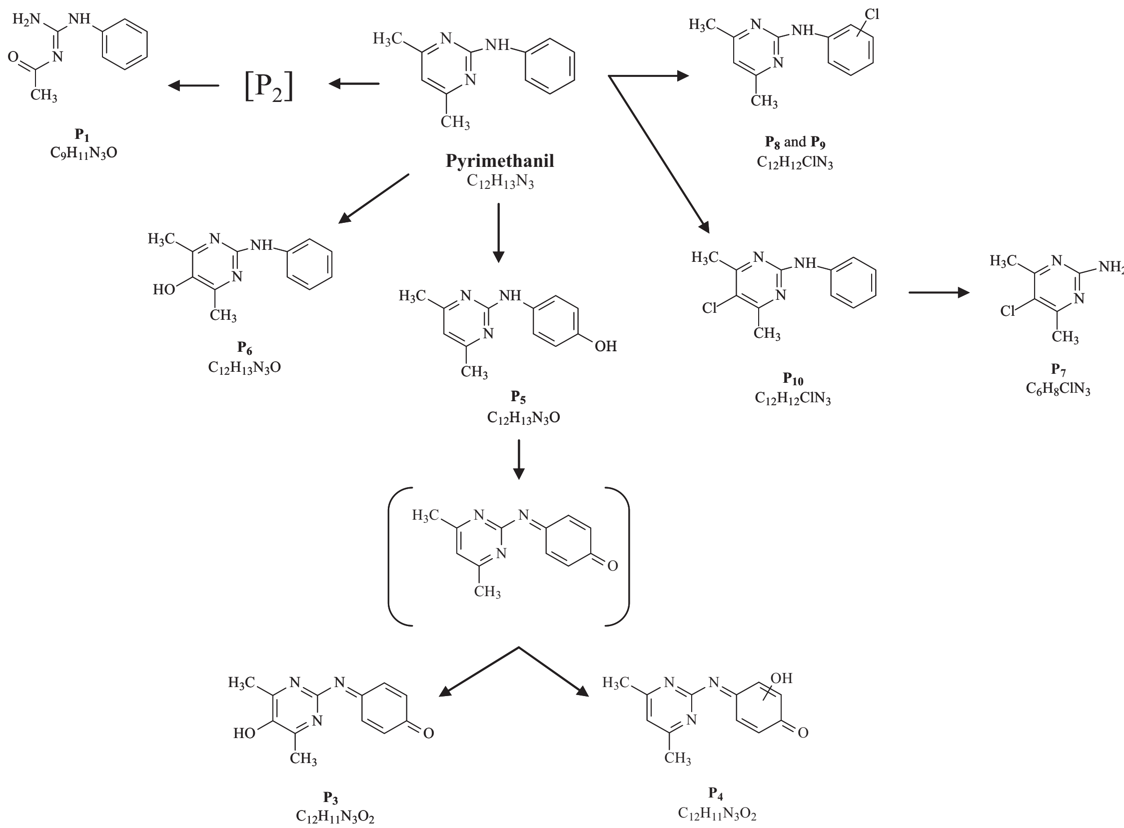


**Scheme 1.** Proposed PYR transformation pathway during photocatalysis in DW (P1–P6) and $DW_{NaCl}$ (P1–P10).

one of the first steps in the degradation process, and yields the formation of the most abundant intermediates. These reactions were observed in both water matrices. Monohydroxylated derivatives had a nominal *m*/*z* 216 for the $[M+H]^+$ ion and an elemental composition of $C_{12}H_{14}N_3O$ without variation from PYR in the DBE. Two compounds (P5 and P6) showed these characteristics with elution at 18.0 and 19.8 min. Two possible structures have been proposed for these compounds. P6 was assigned to hydroxylation in the pyrimidine ring. This position is highly favourable for electrophilic attack because of the higher electron density of the pyrimidine ring. P5 was assigned to hydroxylation in the benzene ring. In this case, a position near the NH substituent would be the most reactive to oxidants (see Scheme 1), as reported in previous publications [18,19].

A total ion chromatogram (TIC) and extracted ion chromatogram (EIC) clearly showed the presence of two TPs with $[M+H]^+$ at *m*/*z* 230. The ion formula in both P3 and P4 was $C_{12}H_{12}N_3O_2$ with a double-bond equivalent of 9, demonstrating that an additional bond had been established. These structures could be a quinone imine derivative formed by oxidation of P5 and subsequent hydroxylation of the resulting molecule at different positions. Evidence of the formation of the quinine imine intermediate was found in the EIC chromatogram, but very little of it, indicating highly favourable hydroxylation of this molecule. Fragmentation of P3 and P4 is useful for assigning the position of the hydroxyl group. Therefore, similarities in the fragmentation spectra of Compounds P3 and P6, which show loss of $-H_2O$ and $-CH_2O$, suggest that the hydroxylation reaction takes place in the pyrimidine ring. On the contrary, P4 shows an ion fragment ($C_6H_7N_2$; *m*/*z* 107) common to the PYR spectrum and attributable to the pyrimidine moiety, thus indicating that hydroxylation occurred in the quinone imine fraction.

P1 has been identified as 2-acetyl(phenyl)guanidine, which is evidence of a parallel route concurrent with hydroxylation due to the attack of the hydroxyl radicals on the C=C double bond in the pyrimidine ring followed by ring opening. The fragmentation pattern found confirms the proposed structure with losses of $-C_2H_2O$ (*m*/*z* 136), corresponding to the acetyl group and $-NH_3$ (*m*/*z* 119). The appearance of the fragment at *m*/*z* 94 ($C_6H_8N$; DBE: 4), corresponding to the aniline moiety also confirms this part of the structure (see Scheme 2). The structure of the compound labelled P2 was not assigned, but was regarded as a TP because its concentration increased and decreased with reaction time. The mass spectrum showed common ions related to P1 (*m*/*z* 136, 119 and 105) thus indicating that P2 corresponds to a previous step in this alternative route.

An additional group of TPs was identified during the experiments in saline water ($DW_{NaCl}$). It is important that all of them had a chlorine atom in their molecule, thus indicating that chlorination reactions can occur during the treatment when wastewater contains a high concentration of chlorine.

Four different chlorinated TPs were unequivocally determined: P7, P8, P9 and P10. Three of them had the same accurate mass (*m*/*z* 233.0720) and elemental composition, $C_{12}H_{13}ClN_3$, but eluted at different retention times, indicating the formation of different isomers. Mass spectra fragmentation (Table 1) showed analogous fragmentation of P8 and P9. This would be related to a similar structure presenting Cl addition in different positions of the aromatic ring. P10 had three fragments common to P7 from a TP identified as 5-chloro-4,6-dimethylpyrimidin-2-amine. It could therefore be concluded that the Cl addition in P10 analogous to P7 was in the "pyrimidine ring" (see Scheme 1).

Figs. 2 and 3 show the most abundant intermediates in both DW and $DW_{NaCl}$ treatment over time. The most abundant by-product generated in DW during treatment was P5 while P4 was found in very low concentrations. All TPs detected were easily degraded during first stages of photo-Fenton (in less than 12 min of illumination).

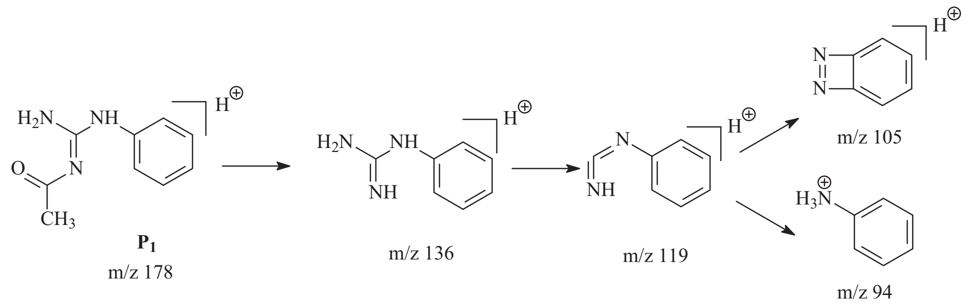


**Scheme 2.** Proposed fragmentation of P1 (2-acetyl(phenyl)guanidine).

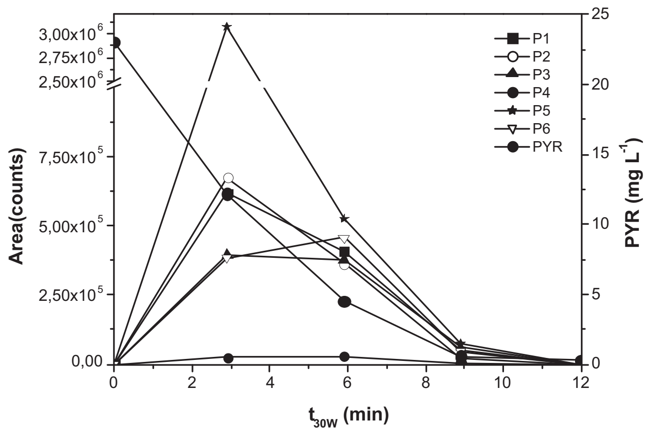


**Fig. 2.** PYR degradation and TPs in DW during photo-Fenton treatment.

In $DW_{NaCl}$, the most abundant TPs were the four chlorinated by-products (P7–P10). P8, P9 and P10 concentrations were the highest at around 6 min of illumination, but fell drastically in the following 20 min. P7 was the most abundant at longer treatment times and turned out to be the most persistent intermediate. P7 disappeared completely only after 65 min of phototreatment. This is of great interest, because it points out the formation of chlorinated intermediates as a relevant issue during the application of advanced oxidation processes to the treatment of saline effluents.

### 3.3. Respirometry assays

Three samples with variable concentrations of PYR and TPs were selected for respirometry analysis to find out the changes in toxicity and biodegradability during the AOP, and any biotransformation of PYR and its TPs.

As described in Section 3.2, even though the structures of the by-products are quite similar to PYR, generally, AOPs (as photo-Fenton) generate more oxidised compounds and biodegradability of more oxidised compounds is usually higher [20]. Besides, it should be remarked that by LC–TOF-MS not all TPs can be identified and therefore more biodegradable compounds could be present and not identified.

The selected samples were the starting solution (M0: 20 mg $L^{-1}$ PYR), and two samples containing large amounts of chlorinated TPs: M1 (6 min of treatment time, 8 mg $L^{-1}$ PYR, high concentrations of P9 and P10) and M2 (10 min of treatment time, 1 mg $L^{-1}$ PYR, and high concentrations of P7 and P9).

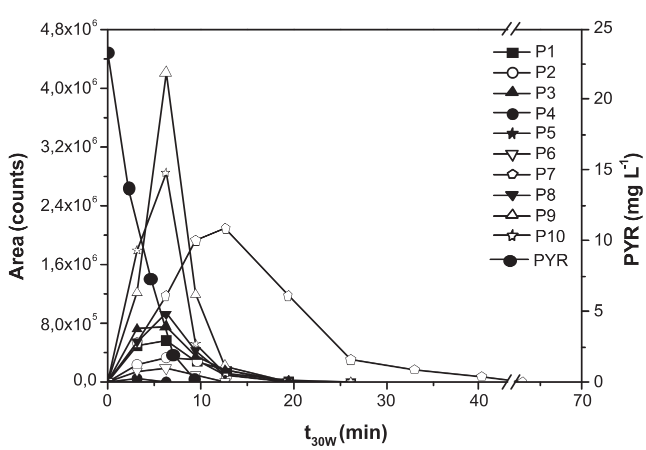


**Fig. 3.** PYR degradation and TPs in $DW_{NaCl}$ during the photo-Fenton treatment.

#### 3.3.1. Toxicity analyses

The toxicity tests in all three samples showed 30% inhibition to activated sludge. It can be concluded that none of the sample results were relevant for biomass, and that the presence of chlorinated TPs did not affect sludge activity.

#### 3.3.2. Biodegradability analyses

Biodegradability analyses were continued 24 h in order to observe any biotransformation of TPs formed during photo-Fenton as it was not expected any biotransformation product of PYR and to evaluate potential chronic toxicity of the samples after exposing biomass to PYR and its TPs. In these tests, each sample (M0, M1 and M2) was individually mixed with the biomass, and after 10 min, two samples were taken from the supernatant and the sludge to find the adsorption of PYR and TPs on the biomass. After 24 h, samples were again taken from the supernatant and the biomass. All samples were analysed by LC–TOF-MS. Throughout the test, oxygen consumption by the biomass was continuously recorded. The most relevant results are summarized below.

M0 (20 mg $L^{-1}$ PYR): After 10 min, 65% of PYR had been adsorbed on the biomass. During the first hours of exposure, no oxygen consumption was recorded, which means that the sample was not rapidly biodegradable. However, after 24 h, the rbCOD/COD ratio was 0.05, demonstrating that after a long enough contact time, PYR can be partially biodegraded.

Regarding the LC–TOF-MS analyses, only PYR was detected in all the samples (supernatant and sludge), suggesting that formation of bio-TPs did not occur.

M1 (6 min of treatment time; 8 mg $L^{-1}$ PYR, P5, P6 $\ll$ P8 < P7 < P9 < P10): 75% of PYR was adsorbed on the biomass after 10 min of exposure. In this case, some oxygen consumption was recorded after 20 min, indicating that at least some of the TPs are easier to biodegrade than PYR. After 24 h, the rbCOD/COD ratio was 0.1, showing a clear increase in biodegradability of the sample with photo-Fenton. According to LC–TOF-MS, PYR, P5, P6 and P7 were detected in both supernatant samples (first and after 24 h). PYR, P8, P9 and P10 were recorded in both sludge samples. PYR and TPs in the samples were lower after 24 h of biotreatment than in the first samples, showing that these compounds can only be partly biodegraded. No formation of bio-TPs was observed.

M2 (10 min treatment time; 1 mg $L^{-1}$ PYR and P7): 60% of PYR was adsorbed on the biomass after 10 min of exposure. Some oxygen consumption was recorded after 10 min of exposure and the rbCOD/COD ratio was 0.2 after 24 h. This also confirms that photo-Fenton increases the biodegradability of PYR.

The LC–TOF-MS analyses found P7 in the four selected samples (supernatant and sludge, first and after 24 h). The final concentration, corresponding to a 30% reduction in P7 after 24 h, was considerably lower than the first. In this case, PYR and P7 were also only partly biodegraded and no new bio-TPs were found.

After 24 h exposure of the biomass to PYR and TPs, sodium acetate (0.5 g/g VSS) was added to evaluate the response of the biomass and find any chronic toxicity. In all three cases (M0, M1 and M2), the biomass respirometric activity was normal, completely consuming the biodegradable substrate (according to the dissolved oxygen recorded). This means that continued exposure of the biomass to PYR and its TPs does not affect sludge activity, corroborating the acute toxicity analyses.

## 4. Conclusions

The formation of chlorinated TPs during photo-Fenton treatment of PYR in water containing high concentrations of chloride has been demonstrated by LC–TOF-MS analysis. Four chlorinated TPs were found during photo-Fenton degradation in the presence of 5 g $L^{-1}$ of NaCl. The chlorinated TPs formed showed greater resistance to photo-Fenton treatment than other TPs. All TPs formed were eliminated during photo-Fenton, demonstrating the efficiency of the phototreatment, for both the elimination of the parent compounds and their main degradation intermediates.

The presence of chlorinated TPs did not increase the toxicity of the water. Furthermore, an increase in biodegradability of the solution was observed as photo-Fenton continued, indicating that the TPs formed are more biodegradable than PYR. LC–TOF-MS revealed that PYR and its TPs formed during photo-Fenton can only be partly biodegraded by activated sludge. No formation of new TPs as a consequence of the biological treatment was observed.

## Acknowledgments

The authors wish to thank the Spanish Ministry of Science and Innovation-FEDER for financial support under the EDARSOL and FOTOREG Projects (references: CTQ2009-13459-C05-01 and CTQ2010-20740-C03-03). Carla Sirtori and Ana Zapata thank the Capes Foundation – Brazil Ministry of Education and the Spanish Ministry of Science and Innovation, respectively, for their Ph.D. research grants.

## References

[1] S. Rodriguez-Mozaz, M.J. López de Alda, D. Barceló, Monitoring of estrogens, pesticides and bisphenol A in natural waters and drinking water treatment plants by solid-phase extraction–liquid chromatography–mass spectrometry, J. Chromatogr. A 1045 (2004) 85–92.

[2] Directive 2000/60/EC of the European Parliament and of the Council of 23 October 2000 establishing a framework for Community action in the field of water policy, The European Parliament and Council, L327/1, 2000.

[3] Directive 2008/105/EC of the European Parliament and of the Council of 23 October 2000 of 16 December 2008, on environmental quality standards in the field of water policy, The European Parliament and Council, L348/84, 2008.

[4] I. Oller, S. Malato, J.A. Sánchez-Pérez., Combination of advanced oxidation processes and biological treatments for wastewater decontamination—a review, Sci. Total Environ. 409 (2011) 4141–4166.

[5] D.J. Hamilton, Á. Ambrus, R.M. Dieterle, A.S. Felsot, C.A. Harris, P.T. Holland, A. Katayama, N. Kurihara, J. Linders, J. Unsworth, S.-S. Wong, Regulatory limits for pesticide residues in water—IUPAC Technical Report, Pure Appl. Chem. 75 (2003) 1123–1155.

[6] J. Kiwi, A. Lopez, V. Nadtochenko, Mechanism and kinetics of the OH-radical intervention during Fenton oxidation in the presence of a significant amount of radical scavenger (Cl−), Environ. Sci. Technol. 34 (2000) 2162–2168.

[7] I. Arslan, I.A. Balcioglu, D.W. Bahnemann, Heterogeneous photocatalytic treatment of simulated dyehouse effluents using novel $TiO_2$-photocatalysts, Appl. Catal. B 26 (2000) 193–206.

[8] N. Barka, S. Qourzal, A. Assabbane, A. Nounah, Y. Ait-Ichou., Factors influencing the photocatalytic degradation of Rhodamine B by $TiO_2$-coated non-woven paper, J. Photochem. Photobiol. A 195 (2008) 346–351.

[9] European Food Safety Authority (EFSA), Conclusion on the peer review of pyrimethanil, Sci. Rep. 61 (2006) 1–70.

[10] I. Oller, S. Malato, J.A. Sánchez-Pérez, M.I. Maldonado, R. Gassó, Detoxification of wastewater containing five common pesticides by solar AOPs–biological coupled system, Catal. Today 129 (2007) 69–78.

[11] A. Zapata, T. Velegraki, J.A. Sánchez-Pérez, D. Mantzavinos, M.I. Maldonado, S. Malato, Solar photo-Fenton treatment of pesticides in water: effect of iron concentration on degradation and assessment of ecotoxicity and biodegradability, Appl. Catal. B 88 (2009) 448–454.

[12] R.F.P. Nogueira, M.C. Oliveira, W.C. Paterlini, Simple and fast spectrophotometric determination of $H_2O_2$ in photo-Fenton reactions using metavanadate, Talanta 66 (2005) 86–91.

[13] M.M.B. Martín, J.L.C. López, I. Oller, S. Malato, J.A.S. Perez, A comparative study of different tests for biodegradability enhancement determination during AOP treatment of recalcitrant toxic aqueous solutions, Ecotoxicol. Environ. Safe. 73 (2010) 1189–1195.

[14] A. Zapata, S. Malato, J.A. Sánchez-Pérez, I. Oller, M.I. Maldonado, Scale-up strategy for a combined solar photo-Fenton/biological system for remediation of pesticide-contaminated water, Catal. Today 151 (2010) 100–106.

[15] J. De Laat, G. Le Truong, Effects of chloride ions on the iron(III)-catalyzed decomposition of hydrogen peroxide and on the efficiency of the Fenton-like oxidation process, Appl. Catal. B 66 (2006) 137–146.

[16] G. Le Truong, J. De Laat, B. Legube, Effects of chloride and sulfate on the rate of oxidation of ferrous ion by $H_2O_2$, Water Res. 38 (2004) 2384–2394.

[17] A. Zapata, I. Oller, E. Bizani, J.A. Sánchez-Pérez, M.I. Maldonado, S. Malato, Evaluation of operational parameters involved in solar photo-Fenton degradation of a commercial pesticide mixture, Catal. Today 144 (2009) 94–99.

[18] L.A. Pérez-Estrada, S. Malato, W. Gernjak, A. Agüera, M. Thurman, I. Ferrer, A.R. Fernández-Alba, Photo-fenton degradation of diclofenac: identification of main intermediates and degradation pathway, Environ. Sci. Technol. 39 (2005) 8300–8306.

[19] S. Othman, V. Mansuy-Mouries, C. Bensoussan, P. Battioni, D. Mansuy, Hydroxylation of diclofenac: an illustration of the complementary roles of biomimetic metalloporphyrin catalysts and yeasts expressing human cytochromes P450 in drug metabolism studies, C. R. Acad. Sci. Paris, Série Iic, Chimie/Chemistry 3 (2000) 751–755.

[20] C. Pulgarín, M. Invernizzi, S. Parra, V. Sarria, R. Polaina, P. Péringer, Strategy for the coupling of photochemical and biological flow reactions useful in mineralization of biocalcitrant industrial pollutants, Catal. Today 54 (1999) 341–352.